Two-Dimensional Pendant Droplet Tensiometry in a Langmuir Monolayer

ARTICLE *in* LANGMUIR · SEPTEMBER 2001

Impact Factor: 4.46 · DOI: 10.1021/la010874e

Two-Dimensional Pendant Droplet Tensiometry in a Langmuir Monolayer

P. Heinig, P. Steffen, S. Wurlitzer, and T. M. Fischer*

Max Planck Institute of Colloids and Interfaces, Am Mühlenberg 1, D-14476 Golm, Germany

Received June 11, 2001. In Final Form: August 2, 2001

The line tension and relative surface potentials of Langmuir monolayer phases are determined in the three-phase coexisting region gas/liquid expanded /liquid condensed of methyl octadecanoate using the pendant droplet technique. The Young−Laplace equation for two-dimensional systems with long-range dipolar interactions is applied to fluorescence images of liquid expanded droplets wetting liquid condensed surfaces in thermodynamic equilibrium. The method yields the line tension of the liquid expanded/gas borderline and the ratio of the surface potentials.

1. Introduction

Pendant drop tensiometry is an accurate method for measuring the interfacial tension of fluid/fluid interfaces.[1] The droplet shape is described by the Young−Laplace equation, a relation between the surface tension, curvature, and pressure difference across the interface. In the present work the pendant drop technique is applied to two-dimensional liquid expanded (LE) droplets immersed in gaseous (G) surroundings and attached to a liquid condensed (LC) region of a methyl octadecanoate Langmuir monolayer (Figures 1 and 2). The asymmetric arrangement of the molecules at the air/water interface leads to electrostatic repulsion between molecular dipoles (oriented perpendicular to the surface) and to long-range interactions of the droplet with the surroundings and the droplet. A simple Landau free energy has been used successfully to describe a rich variety of effects caused by these long-range interactions both in Langmuir monolayers[2] and in ferrofluids. The description has been extended to dynamical equations[3,4] to describe the evolution of nontrivial patterns. In contrast to systems with short-range interactions, the effective line tension and Laplace pressure, defined as the functional derivatives of the Landau free energy F of the droplet

$$\lambda_{\text{eff}}[\mathbf{r}(s), \delta\mathbf{r}(s)] = \frac{\delta F}{\delta P}|_A \tag{1}$$

and

$$p[\mathbf{r}(s), \delta\mathbf{r}(s)] = -\frac{\delta F}{\delta A}|_P \tag{2}$$

depend on the shape $\mathbf{r}(s)$ and the mode of deformation $\delta\mathbf{r}(s)$ (s denotes the arc length of the droplet boundary, A the area and P the total length of the phase boundary). This shape dependency of the effective line tension causes shape transitions from circular to $n = 2, 3, \ldots$ -fold symmetric shapes,[3,6−8] wetting/dewetting transitions,[11,12] and structure-dependent contact angles.[11,12] An effective line tension of a droplet that does not state the mode of deformation $\delta\mathbf{r}(s)$ (with droplet borderline $\mathbf{r}(s)$) has no physical meaning in these droplets. The Young−Laplace law is an equation involving the equilibrium shape $\mathbf{r}(s)$ of the droplet and is independent of the deformation modes $\delta\mathbf{r}(s)$. For reasons of consistency with the linear response type definitions in eqs 1 and 2, a whole spectrum of deformation mode independent (non response type) line tensions of such a droplet should enter the Young−Laplace equation. It has been shown by Rivière et al.,[9] that in the Young−Laplace equation of a droplet with dipole−dipole interactions the short-range component of the dipolar interactions can be included into a renormalized line tension (note that this line tension is a materials parameter and is independent of the mode of deformation) and the long-range component into the Laplace pressure. The choice of length scale a dividing between short and long-range components is arbitrary. This ambiguity reflects the fact that the resistance of the droplet with respect to elongations of its perimeter varies with the mode of elongation. If the dividing length scale between short- and long-range components is kept small in comparison to the radius of curvature of the droplet, then a simple scaling law of the line tension and Laplace pressure with the dividing length scale applies which greatly simplifies the evaluation of experimental droplet shapes.

The present work will make use of such scaling laws in order to determine the bare line tension and the ratio of the surface potentials of the different 2d liquids from the droplet shape.

2. Theoretical Model

Within a 2d system, consider a 2d LE droplet wetting a LC/G interface (Figure 1). The interfaces between the phases are characterized by the bare line tensions $\lambda_{\text{LE/G}}$, $\lambda_{\text{LE/LC}}$ and $\lambda_{\text{LC/G}}$, the phases by bare surface pressures p_{G}, p_{LE} and p_{LC}, hypothetical quantities valid in the limit of

* Corresponding author. E-mail: thomas.fischer@mpikg-golm.mpg.de.

(1) Ambwani, D.; Fort, T. *Surf. Colloid Sci.* **1979**, *11*, 93.
(2) McConnell, H. M. *Annu. Rev. Phys. Chem.* **1991**, *42*, 171.
(3) Langer, S. A.; Goldstein, R. E.; Jackson, D. P. *Phys. Rev. A* **1992**, *46*, 4894.
(4) Stone, H. A.; McConnell, H. M. *Proc. R. Soc. London A* **1995**, *448*, 97.
(5) McConnell, H. M.; de Koker, R. *J. Phys. Chem.* **1992**, *96*, 7101.
(6) Vanderlick, T. K.; Möhwald, H. *J. Phys. Chem.* **1990**, *94*, 886.
(7) de Koker, R.; McConnell, H. M. *J. Phys. Chem.* **1993**, *97*, 13419.
(8) Lee, K. Y. C.; McConnell, H. M. *J. Phys. Chem.* **1993**, *97*, 9532.
(9) Rivière, S.; Henon, S.; Meunier, J.; Albrecht, G.; Boissonade, M. M.; Baszkin, A. *Phys. Rev. Lett.* **1995**, *75*, 2506.
(10) Heinig, P.; Wurlitzer, S.; Steffen, P.; Kremer, F.; Fischer, Th. M. *Langmuir* **2000**, *16*, 10254.
(11) Khattari, Z.; Heinig, P.; Wurlitzer, S.; Steffen, P.; Lösche, M.; Fischer, Th. M. Submitted for publication.
(12) Heinig, P.; John, Th.; Fischer, Th. M. Shapes of spreading two-dimensional droplets. Manuscript in preparation.

10.1021/la010874e CCC: $20.00
Published on Web 09/20/2001

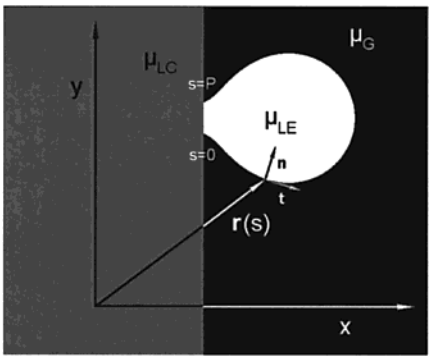

Figure 1. Schematic illustration of a two-dimensional pendant droplet in a Langmuir monolayer. A white LE droplet is attached to a boundary between a solid gray LC phase and a dark gaseous phase. The droplet of bare line tension $\lambda_{LE/G}$ is deformed from a circular segment shape due to electrostatic interactions of the LE phase ($\mu = \mu_{LE}$) with itself, with the gaseous ($\mu = \mu_G$) and solid LC phases ($\mu = \mu_{LC}$). The aim of this work is to determine the line tension $\lambda_{LE/G}$ from the shape $\mathbf{r}(s)$ of the LE/G facet of length P of the droplet.

vanishing dipolar contributions. One may write the Landau free energy of the monolayer as a sum of line, bulk, and electrostatic energies:[5]

$$F = \sum_{i,j} F_{el}^{ij} + F_b + F_\lambda \tag{3}$$

The three types of energies are as follows:[5] The dipolar energy between the domains of the phases i and j

$$F_{el}^{ij} = \frac{\mu_i \mu_j}{2} \int_{A_i} \int_{A_j} \frac{dA\, dA'}{\rho^3} \quad with \quad \rho = \sqrt{(\mathbf{r} - \mathbf{r}')^2 + \Delta^2} \tag{4}$$

where A_i (A_j) is the area occupied by phase i (j) and Δ is a cutoff length of molecular dimension below which the dipole forces are screened by other interactions within the monolayer.[5] The line energy F_λ of a droplet is proportional to the length of the borderline between the domains of phases i and j and to the bare line tension λ_{ij}

$$F_\lambda = \sum_{i \le j} \lambda_{ij} \int_{\partial A_i \cap \partial A_j} ds \tag{5}$$

and the bulk free energy satisfies

$$dF_b = -\sum_i p_i\, dA_i \tag{6}$$

with p_i the bare surface pressure within the domain of area A_i. We will consider liquid expanded droplets embedded into a gaseous phase and therefore the dipole density difference μ_{iG} between phase i and the gaseous phase (j = G) is defined by[9]

$$\mu_{iG}^2 = (\mu_i - \mu_G)^2 = \frac{\epsilon_0}{4\pi} \frac{2\epsilon_w \epsilon_{air}}{\epsilon_w + \epsilon_{air}} (V_i - V_G)^2, \tag{7}$$

where ϵ_{air} (ϵ_w) denotes the relative permittivity of air (water) and V_i the surface potential of phase i. The Young−Laplace equation is obtained from eqs 3−6 by minimizing the Landau free energy (eq 3) with respect to variations

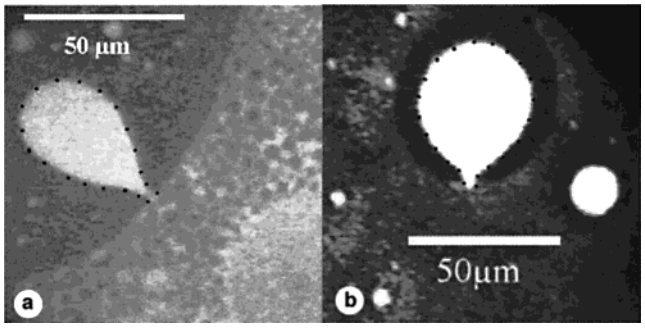

Figure 2. Pendant droplets in the three-phase coexistence region LE (bright), LC (gray), and gas (dark) of a methyl octadecanoate monolayer. The interaction parameters $\tilde{\mu}$ and $\tilde{\lambda}$ are calculated from the geometry of the images using the Young−Laplace equation: (a) pendant droplet at $A_{mol} = 30$ Å^2 attached to a straight LC wall; (b) pendant droplet of a denser monolayer ($A_{mol} = 25$ Å^2) formed in a circular gas bubble

of the droplet shape. The resulting Euler−Lagrange equation (Appendix A) reads

$$p = \sum_i \mu_{LE/G} \mu_{i/G} \oint_{\partial A_i} \frac{\mathbf{n}' \cdot (\mathbf{r} - \mathbf{r}')}{\Delta(\rho + \Delta)\rho} ds' + \lambda_{LE/G} \kappa(s) \tag{8}$$

where $\kappa(s)$ is the curvature of the droplet interface at the point defined by the arc length s and $p = p_{LE} - p_G$ is the bare Laplace pressure. The summation of the electrostatic contribution is done over all boundaries ∂A_i. To avoid divergencies in the numerical treatment of the integral in eq 8, which occur in the limit $\Delta \to 0$, we introduce a length scale a with $\kappa\Delta \ll \kappa a \ll 1$, and one finds to the leading order of Δ (Appendix B):

$$p - \frac{\pi \mu_{LE/G}^2}{\Delta} = - \sum_i \mu_{LE/G} \mu_{i/G} \oint_{\partial A_i} ds' \frac{\mathbf{n}' \cdot (\mathbf{r} - \mathbf{r}')}{(\mathbf{r} - \mathbf{r}')^2 \sqrt{(\mathbf{r} - \mathbf{r}')^2 + a^2}} + \left(\lambda_{LE/G} - \mu_{LE/G}^2 \ln \frac{a}{\Delta} \right) \kappa(s) \tag{9}$$

Equation 9 is a relation between the curvature $\kappa(s)$, the line tension $\lambda_{LE/G}$, and the electrostatic pressure or bare Laplace pressure p, respectively, i.e., the Young−Laplace equation for the 2d system with dipolar interaction. From eq 9 one deduces that if one has found a solution of the Young−Laplace equation to the set of parameters (λ, p, μ_i, Δ), then it is also a solution for the parameters $\lambda^*_{LE/G} = \lambda_{LE/G} - \mu_{LE/G}^2 \ln(\Delta^*/\Delta)$, $p^* = p - \mu_{LE/G}^2(\pi/\Delta - \pi/\Delta^*)$, $\mu_i^* = \mu_i$, and Δ^*.

3. Fluorescence Microscopy and Droplet Shape Analysis

A monolayer of methyl octadecanoate is observed using fluoresence microscopy adding 1% of NBD-HDA fluorescence label. The different phases can be distinguished by their fluorescence intensity. Methyl octadecanoate is spread on Millipore water to an area per molecule of $A_{mol} = 25-30$ Å^2 at a temperature of 25 °C. Under these conditions the phases LC (gray), LE (bright), and G (dark) coexist. After expansion to $A_{mol} \approx 100$ Å^2 and recompression, two-dimensional pendant LE droplets on LC borderlines occur. Two fluorescence microscopy images of such droplets are shown in Figure 2. Figure 2a shows a droplet

at an area per molecule of $A_{mol} = 30$ Å^2. The droplet curvature changes as one moves along its LE/G boundary. Close to the points where the droplet is attached to the LC phase, the curvature is negative with a concave droplet shape. About 20 μm from the LC phase, the curvature changes sign and the droplet is convex with a radius of curvature of roughly 20 μm. The droplet partially wets an extended LC region. The characteristic shape of the droplet is a result of the interplay of the line tension, the electrostatic self-interaction, and the electrostatic repulsion from the LC phase to which the droplet is attached. Figure 2b is taken at an area per molecule of $A_{mol} = 25$ Å^2, where the droplets are confined to circular gas cavities. Its shape is closer to a circle than that of Figure 2b. The change in sign of the droplet curvature occurs much closer ($\approx 5\,\mu$m) to the LC boundary than that of the less confined droplet. The fluorescence images of pendant droplets were videotaped and digitized for further analysis.

The integrals in eq 9 can be separated into interactions of the droplet with the LE regions:

$$I_{LE} = -\int_{\partial A_{LE}} ds' \frac{\mathbf{n}'\cdot(\mathbf{r}-\mathbf{r}')}{(\mathbf{r}-\mathbf{r}')^2\sqrt{(\mathbf{r}-\mathbf{r}')^2 + a^2}} \qquad (10)$$

and into interactions of the droplet with the LC regions:

$$I_{LC} = -\int_{\partial A_{LC}} ds' \frac{\mathbf{n}'\cdot(\mathbf{r}-\mathbf{r}')}{(\mathbf{r}-\mathbf{r}')^2\sqrt{(\mathbf{r}-\mathbf{r}')^2 + a^2}} \qquad (11)$$

where the integration is performed over all LE (LC) boundaries in the monolayer. All tangent vectors $\mathbf{t}'$ are chosen such that the LE (LC) phase is to the left and $\mathbf{n}'$ is pointing into the LE (LC) phase. The boundaries are taken from the image and approximated by cubic splines traveling through sampling points set at a separation of approximately 5 μm. The integrals I_{LE} and I_{LC} in eqs 10 and 11 are determined by numerical integration. The parameter a is arbitrary and has been set to $a = 10$ pixels, $\approx 4\,\mu$m larger than the step width (0.4 μm) in the numerical integration procedure.

Equation 9 yields an overdetermined linear system of equations, since it has to be fulfilled at every sampling point $\mathbf{r}(s_i)$, $i = 1, 2, 3, ..., N$, at the LE/G droplet boundary.

$$\tilde{\mu} I_{LE}(s_i) + I_{LC}(s_i) + \tilde{\lambda}\kappa(s_i) = \tilde{p} \qquad (12)$$

In eq 12, the integrals I_{LE}, I_{LC}, and κ are geometrical quantities determined from the fluorescence images while the renormalized dimensionless pressure

$$\tilde{p} = \frac{p - \frac{\pi \mu_{LE/G}^2}{\Delta}}{\mu_{LE/G}\mu_{LC/G}} \qquad (13)$$

the renormalized dimensionless line tension

$$\tilde{\lambda} = \frac{\lambda_{LE/G} - \mu_{LE/G}^2 \ln\frac{a}{\Delta}}{\mu_{LE/G}\mu_{LC/G}} \qquad (14)$$

and the ratio between the relative surface potentials

$$\tilde{\mu} = \frac{\mu_{LE/G}}{\mu_{LC/G}} \qquad (15)$$

are the unknown material parameters. One can eliminate

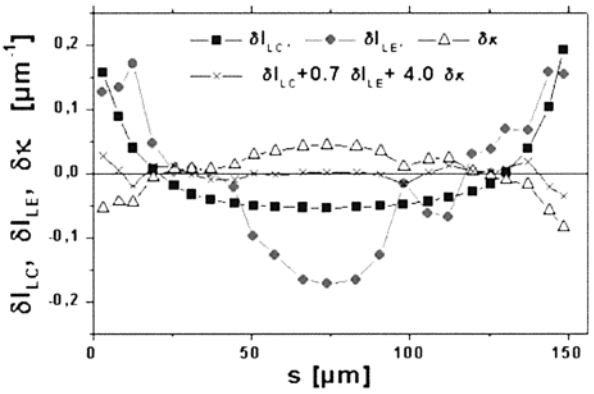

Figure 3. Plot of the integrals $\delta I_{LC}(s)$, $\delta I_{LE}(s)$, $\delta\kappa(s)$, and $\delta I_{LC}(s) + \tilde{\mu}\delta I_{LE}(s) + \tilde{\lambda}\delta\kappa(s)$, ($\tilde{\mu} = 0.7$, $\tilde{\lambda} = 4$) along the boundary of the droplet presented in Figure 2a. The deviation of the latter sum from zero is about 10% of the size of the first three graphs, and the error in $\tilde{\lambda}$ for this individual droplet is also around 10%.

$\tilde{p}$ in eq 12 by introducing the fluctuations

$$\delta f(s_i) = f(s_i) - \frac{1}{N}\sum_j f(s_j) \qquad (16)$$

to find

$$\tilde{\mu}\delta I_{LE}(s_i) + \tilde{\lambda}\delta\kappa(s_i) = -\delta I_{LC}(s_i) \qquad (17)$$

The two parameters $\tilde{\lambda}$ and $\tilde{\mu}$ are determinded by applying a least-squares procedure to eq 17.

In Figure 3, we show the integrals $\delta I_{LE}(s)$, $\delta I_{LC}(s)$, and $\delta\kappa(s)$ as well as $\tilde{\mu}\delta I_{LE}(s) + \delta I_{LC}(s) + \tilde{\lambda}\delta\kappa(s)$ as a function of the position s along the LE/G boundary for the droplet in Figure 2a. As one can see, the least-squares deviations are approximately 10% of the values of the integrals, and errors are of the same order of magnitude. The least-squares procedure is more accurate for the determination of $\tilde{\lambda}$ than for $\tilde{\mu}$. We applied the least-squares procedure to 14 different LE droplets. The results are $\tilde{\mu} = 0.26 \pm 0.12$ and $\tilde{\lambda} = 3.3 \pm 0.2$, which with $\Delta = 5$ Å,[5] $V_{LC} - V_G = 0.41 \pm 0.01$ V, and $V_{LE} - V_G = 0.15 \pm 0.03$ V[10] is equivalent to $\lambda_{LE/G} = (0.6 \pm 0.2)$pN.

4. Discussion and Conclusion

The Young−Laplace equation is derived under assumption of homogeneous phases. It has been shown by Pandit and Fischer[17] that in the vicinity of and at a three-phase coexistence, the bulk properties may be modified near phase boundaries. This may effect the shape of the interface and therefore the measured line tension and surface potentials. The comparison of the ratio of the surface potentials ($\tilde{\mu} = 0.26$) and the value measured in the system before[10] ($\tilde{\mu} = 0.35$) point toward a decrease of the surface potential near the phase boundary.

Line tensions in Langmuir monolayers have been measured by Muller et al.[14] ($\lambda = 5$ pN), Benvegnu et al.[13] ($\lambda = 1.5$ pN), Rivière et al. ($\lambda = 0.7$ pN) in different systems and by Wurlitzer et al. in methyl octadecanoate ($\lambda_{LE/LC} =$

(13) Benvegnu, D. J.; McConnell, H. M. *J. Phys. Chem.* **1992**, *96*, 6820.
(14) Muller, P.; Gallet, F. *Phys. Rev. Lett.* **1991**, *67*, 1106.
(15) Wurlitzer, S.; Steffen, P.; Wurlitzer, M.; Khattari, Z.; Fischer, Th. M. *J. Chem. Phys.* **2000**, *113*, 3822.
(16) Wurlitzer, S.; Steffen, P.; Fischer, Th. M. *J. Chem. Phys.* **2000**, *112*, 5915.
(17) Pandit, R.; Fisher, M. E. *Phys. Rev. Lett.* **1983**, *51*, 1772.
(18) Benvegnu, D. J.; McConnell, H. M. *J. Phys. Chem.* **1993**, *97*, 6686.

7.5 pN[15] and $\lambda_{LE/G} = 0.5$ pN[16]). All values are of the same order of magnitude, and the value obtained by Wurlitzer et al. for the LE/G tension using a hydrodynamic technique is in excellent agreement with the pendant droplet technique employed in this work. This shows, that the electrostatics, hydrodynamics and thermodynamics of the system is treated consistently.

The method precisely determines the quantity $\tilde{\lambda}$.[14] In the conversion to the line tension $\lambda_{LE/G} = 0.6 \pm 0.2$ pN, however, large errors are introduced due to the uncertainty of the surface potentials and the line tension is determined less accurate than using hydrodynamic[13,15,16] techniques. The pendant droplet technique is especially useful for the measurement of low line tensions (large LC surface potential), where the droplet shape deviates from a circular segment.

Acknowledgment. We thank Prof. Möhwald for generous support and stimulating discussion, and T.M.F. thanks the German Science Foundation for providing a Heisenberg fellowship. This work is supported by the German Science Foundation within the priority program *wetting and structure formation at interfaces*.

Appendix A: Young−Laplace Equation of a 2d System with Dipolar Interaction

First we convert the interaction integrals in eq 4 into line integrals, using the identity

$$\nabla' \cdot \nabla \frac{\ln(\rho + \Delta)}{\Delta} = -\frac{1}{\rho^3} \tag{A1}$$

and Green's theorem

$$\int_A \nabla \Phi \, dA = -\sum_{\partial A} \mathbf{n} \Phi \, ds. \tag{A2}$$

($\mathbf{n}$ is the *inward* normal vector to the area A, cf. (4).) Equation 4 transforms into

$$F = -\sum_{f_{ij}, f_{kl}} \frac{(\mu_i - \mu_j)(\mu_k - \mu_l)}{2\Delta} \int_{f_{ij}} ds \int_{f_{kl}} ds' \, \mathbf{n} \cdot \mathbf{n}' \ln(\rho + \Delta) + F_b + \sum_{f_{ij}} \lambda_{ij} \int_{f_{ij}} ds \tag{A3}$$

where f_{ij} are the facets between phase i and j and $\mathbf{n}(s)$ is the normal vector to the boundary defined by the fundamental relations

$$\frac{d\mathbf{r}(s)}{ds} = \mathbf{t}(s), \quad \frac{d\mathbf{t}(s)}{ds} = \kappa \mathbf{n}(s), \quad \text{and} \quad \frac{d\mathbf{r}(s)}{ds} = -\kappa \mathbf{t}(s) \tag{A4}$$

The free energy (eq A3) of the droplet with area

$$A = -\frac{1}{2} \int_{f_{D/G}} \mathbf{r} \cdot \mathbf{n} \, ds - \frac{1}{2} \int_{f_{D/LC}} \mathbf{r} \cdot \mathbf{n} \, ds \tag{A5}$$

is a function of $\mathbf{r}$, $\mathbf{t}$, and $\mathbf{n}$. The normal vector $\mathbf{n}$ and tangent vector $\mathbf{t}$ are related by a rotation of $\pi/2$: $\sigma \mathbf{t} = \mathbf{n}$, $\sigma^2 = -1$, and $\sigma^t = -\sigma$. Eliminating $\mathbf{n}$ in eq 3 we arrive at

$$F = -\sum_{f_{ij}, f_{kl}} \frac{(\mu_i - \mu_j)(\mu_k - \mu_l)}{2\Delta} \int_{f_{ij}} ds \int_{f_{kl}} ds' \, \mathbf{t} \cdot \mathbf{t}' \ln(\rho + \Delta) + F_b + \sum_{f_{ij}} \lambda_{ij} \int_{f_{ij}} ds \tag{A6}$$

We wish to minimize F with respect to the LE/G boundary of the droplet $\mathbf{r}_{D/G}(s)$ resulting in the Euler−Lagrange equation

$$\frac{\delta F}{\delta \mathbf{r}_{D/G}(s)} - \frac{d}{ds} \frac{\delta F}{\delta \dot{\mathbf{r}}_{D/G}(s)} = 0 \tag{A7}$$

where $\dot{\mathbf{r}}_{D/G}(s) = \mathbf{t}_{D/G}(s)$. Using eqs A6, A5, and 6, the individual derivatives are

$$\frac{\delta F}{\delta \mathbf{r}(s)} = \sum_{f_{ij}} \frac{\mu_{LE/G}(\mu_i - \mu_j)}{\Delta} \int_{f_{ij}} \frac{(\mathbf{t} \cdot \mathbf{t}')}{\rho(\rho + \Delta)} (\mathbf{r} - \mathbf{r}') \, ds' +$$

$$\frac{p}{2} \mathbf{n} \frac{d}{ds} \frac{\delta F}{\delta \mathbf{t}(s)} = -\sum_{f_{ij}} \frac{\mu_{LE/G}(\mu_i - \mu_j)}{\Delta} \int_{f_{ij}} \frac{(\mathbf{t} \cdot (\mathbf{r} - \mathbf{r}'))}{\rho(\rho + \Delta)} \mathbf{t}' \, ds' - \frac{p}{2} \mathbf{n} + \lambda_{LE/G} \kappa \mathbf{n}$$

where we have dropped the index D/G on $\mathbf{r}$ and $\mathbf{t}$. Finally using the identity

$$(\mathbf{t} \cdot \mathbf{t}')(\mathbf{r} - \mathbf{r}') - ((\mathbf{r} - \mathbf{r}') \cdot \mathbf{t}) \mathbf{t}' = (\mathbf{n}' \cdot (\mathbf{r} - \mathbf{r}')) \mathbf{n} \tag{A8}$$

the Euler−Lagrange equation reads

$$p = \sum_{f_{ij}} \mu_{LE/G}(\mu_i - \mu_j) \int_{f_{ij}} \frac{\mathbf{n}' \cdot (\mathbf{r} - \mathbf{r}')}{\Delta(\rho + \Delta)\rho} ds' + \lambda_{LE/G} \kappa \tag{A9}$$

where the summation is taken over all facets in the fluorescence microscopy image. Collecting terms proportional to $\mu_{LE/G}^2$ and $\mu_{LE/G} \mu_{LC/G}$ we obtain (8).

Appendix B: Scaling Laws

One finds for the integral in (8)

$$\oint \frac{\mathbf{n}' \cdot (\mathbf{r} - \mathbf{r}')}{\Delta(\rho + \Delta)\rho} ds' = \oint \frac{\mathbf{n}' \cdot (\mathbf{r} - \mathbf{r}')}{\Delta(\mathbf{r} - \mathbf{r}')^2} ds' - \oint \frac{\mathbf{n}' \cdot (\mathbf{r} - \mathbf{r}')}{\rho(\mathbf{r} - \mathbf{r}')^2} ds' \tag{B1}$$

The first integral on the right side of eq B1 can be solved:

$$\oint \frac{\mathbf{n}' \cdot (\mathbf{r} - \mathbf{r}')}{\Delta(\mathbf{r} - \mathbf{r}')^2} ds' = -\int dA' \, \nabla' \frac{(\mathbf{r} - \mathbf{r}')}{\Delta(\mathbf{r} - \mathbf{r}')^2} = \int dA' \, \frac{2\pi}{\Delta} \delta_{Dirac}(\mathbf{r} - \mathbf{r}') = \frac{\pi}{\Delta} \tag{B2}$$

Note that $\mathbf{r}$ lays on the border of A'. Introducing a length scale $\kappa\Delta \ll \kappa a \ll 1$ the right integral on the right side of (1) can be written as

$$\oint ds' \frac{\mathbf{n}' \cdot (\mathbf{r} - \mathbf{r}')}{\rho(\mathbf{r} - \mathbf{r}')^2} = \oint ds' \frac{\mathbf{n}' \cdot (\mathbf{r} - \mathbf{r}')}{(\mathbf{r} - \mathbf{r}')^2} \left(\frac{1}{\rho} \frac{1}{\rho_a} \right) + \oint ds' \frac{\mathbf{n}' \cdot (\mathbf{r} - \mathbf{r}')}{\rho_a (\mathbf{r} - \mathbf{r}')^2} \tag{B3}$$

with

$$\rho_a = \sqrt{(\mathbf{r} - \mathbf{r}')^2 + a^2} \tag{B4}$$

$\rho^{-1} - \rho_a^{-1}$ is a function peaked at $\mathbf{r} - \mathbf{r}' = \mathbf{0}$ of width a.

The first integral on the right side of (B3) can be evaluated by expanding the prefactor $\mathbf{n}'\cdot(\mathbf{r} - \mathbf{r}')/(\mathbf{r} - \mathbf{r}')^2$ using

$$\mathbf{r} = \mathbf{r}' + (s - s')\mathbf{t}' + \frac{\kappa'}{2}(s - s')^2\mathbf{n}'; (\mathbf{r} - \mathbf{r}')^2 = (s - s')^2 \tag{B5}$$

and one obtains

$$\oint ds'\frac{\mathbf{n}'\cdot(\mathbf{r} - \mathbf{r}')}{(\mathbf{r} - \mathbf{r}')^2}\left(\frac{1}{\rho} - \frac{1}{\rho_a}\right) \approx \int_{-\infty}^{\infty} ds'\,\frac{\kappa(s')}{2}\left(\frac{1}{\sqrt{(s - s')^2 + \Delta^2}} - \frac{1}{\sqrt{(s - s')^2 + a^2}}\right) \tag{B6}$$

$$\approx \frac{\kappa(s)}{2}\int_{-\infty}^{\infty} ds'\left(\frac{1}{\sqrt{(s - s')^2 + \Delta^2}} - \frac{1}{\sqrt{(s - s')^2 + a^2}}\right) = -\kappa(s)\ln\frac{\Delta}{a} \tag{B7}$$

combining (B2), (B3), and (B6), we find

$$\oint\frac{\mathbf{n}'\cdot(\mathbf{r} - \mathbf{r}')}{\Delta(\rho + \Delta)\rho}ds' = \frac{\pi}{\Delta} - \kappa(s)\ln\frac{a}{\Delta} - \oint\frac{\mathbf{n}'\cdot(\mathbf{r} - \mathbf{r}')}{\rho_a(\mathbf{r} - \mathbf{r}')^2}ds' \tag{B8}$$

Inserting (B8) into (8) results in (9).

LA010874E